DALTON
FULL PAPER

# Spectroelectrochemistry of potassium ethylxanthate, bis(ethylxanthato)nickel(II) and tetraethylammonium tris(ethylxanthato)-nickelate(II) †

**Ömer Dag,‡ Seniz Özalp Yaman,§ Ahmet M. Önal * and Huseyin Isci ***

*Department of Chemistry, Middle East Technical University, 06531 Ankara, Turkey*

***Received 28th June 2001, Accepted 31st July 2001***
***First published as an Advance Article on the web 12th September 2001***

Electrochemical and chemical oxidation of $S_2COEt^-$, $Ni(S_2COEt)_2$, and $[Ni(S_2COEt)_3]^-$ have been studied by CV and *in situ* UV-VIS spectroscopy in acetonitrile. Cyclic voltammograms of $S_2COEt^-$ and $Ni(S_2COEt)_2$ display one (0.00 V) and two (0.35 and 0.80 V) irreversible oxidation peaks, respectively, referenced to an $Ag/Ag^+$ (0.10 M) electrode. However, the cyclic voltammogram of $[Ni(S_2COEt)_3]^-$ displays one reversible (−0.15 V) and two irreversible (0.35, 0.80 V) oxidation peaks, referenced to an $Ag/Ag^+$ electrode. The low temperature EPR spectrum of the oxidatively electrolyzed solution of $(NEt_4)[Ni(S_2COEt)_3]$ indicates the presence of $[Ni^{III}(S_2COEt)_3]$, which disproportionates to $Ni(S_2COEt)_2$, and the dimer of the oxidized ethylxanthate ligand, $(S_2COEt)_2$ ($(S_2COEt)_2$ = $C_2H_5OC(S)SS(S)COC_2H_5$), with a second order rate law. The final products of constant potential electrolysis at the first oxidation peak potentials of $S_2COEt^-$, $Ni(S_2COEt)_2$, and $[Ni(S_2COEt)_3]^-$ are $(S_2COEt)_2$; $Ni^{2+}$(sol) and $(S_2COEt)_2$; and $Ni(S_2COEt)_2$ and $(S_2COEt)_2$, respectively. The chemical oxidation of $S_2COEt^-$ to $(S_2COEt)_2$, and $[Ni(S_2COEt)_3]^-$ to $(S_2COEt)_2$ and $Ni(S_2COEt)_2$ were also achieved with iodine. The oxidized ligand in the dimer form can be reduced to $S_2COEt^-$ with $CN^-$ in solution.

## Introduction

The chemistry of nickel is mostly centered on its "+2" oxidation state with $d^8$ electron configuration. Octahedral complexes are paramagnetic, $S = 1$, and square-planar complexes are diamagnetic, $S = 0$. In spite of the fact that Ni(I), $d^9$, and Ni(III), $d^7$, were reported as early as 1913 ($K_4[Ni_2(CN)_6]$) and 1936 ($[Ni(PEt_3)_2Br_3]$),[1] the interest in the chemistry of Ni(I) and Ni(III) started after the discovery of nickel as a bioessential trace element in several important enzymes in the 1970s.[2] Today the presence of nickel has been demonstrated in urease, hydrogenase, CO oxidoreductase, and methyl-coenzyme M reductase enzymes.[3–5] Detailed structural information on the geometry and coordination of the nickel in these enzymes is very important for understanding the mechanism of catalysis. A study on the crystal structure of nickel–iron hydrogenase from *Desulfovibrio gigas* indicated that the active site contains nickel coordinated to four sulfur donor ligands with a geometry between square-planar and tetrahedral.[6] EPR studies on several nickel containing enzymes isolated from bacteria suggested that during the catalytic turnover nickel changes its oxidation state from $Ni^I$ to $Ni^{II}$ to $Ni^{III}$.[3] Thus, the activity of the nickel center in these enzymes is attributed to its redox chemistry. Unless the coordination environment is known, it is not possible to distinguish Ni(I) from Ni(III) by using EPR data. The possibility of antiferromagnetic coupling of paramagnetic nickel with the [4Fe–4S] cluster complicates the issue even further.[7]

In the last two decades a great deal of research effort has been directed towards the synthesis of complexes of Ni(I) and Ni(III),[1,8–16] which can serve as models to further our understanding of this metal in biological systems. Polypeptides,[17,18] tetraaza macrocycles,[11] dioximes, and deprotonated amide ligands are reported to be effective in stabilizing Ni(III). Studies of the nickel complexes with sulfur donor ligands are also important in view of the fact that nickel is coordinated to sulfur atoms in hydrogenase enzymes. Up to now the redox behavior of Ni(II) complexes with 1,2-dithiolates,[9–21] dithiocarbamates,[8,22] and thioether ligands,[23] have been studied in considerable detail. In the case of 1,2-dithiolate complexes the redox is centered on the ligands and no changes took place in the metal oxidation state. With other ligands, the formation [12–14,16] and the isolation [24–26] of Ni(III) complexes were reported.

The studies on redox properties of nickel complexes with xanthates and thioxanthates, which are good ligands for nickel, are limited. Hendrickson *et al.*[8] reported that the electrochemical oxidation of $[Ni(S_2COEt)_3]^-$ yielded $[Ni^{III}(S_2COEt)_3]$. More recently, Chakravorty and co-workers investigated the electrochemical behavior of $[Ni(S_2COR)_3]^-$ (R = $CH_3$, $C_2H_5$, n-$C_3H_7$, n-$C_4H_9$ and i-$C_4H_9$) complexes.[27] From the low temperature EPR measurement they claimed that electrochemical oxidation of $[Ni(S_2COEt)_3]^-$ indeed led to the formation of $[Ni^{III}(S_2COEt)_3]$, in which the nickel is in its "+3" oxidation state.

In this work we studied electrochemical and chemical oxidation of $S_2COEt^-$, $Ni(S_2COEt)_2$, and $[Ni(S_2COEt)_3]^-$ in acetonitrile. First we measured the cyclic voltammogram of each species using an $Ag/Ag^+$ reference electrode, then carried out constant potential electrolysis at their lowest oxidation peak potentials. Since the quantitative electronic absorption spectra are known,[28] the changes in the UV-VIS absorption spectra are followed *in situ* during the electrolysis to identify the oxidation products. *In situ* EPR spectra were measured in order to detect any radical intermediates.

## Experimental

The ligand $K(S_2COEt)$ and the complexes $Ni(S_2COEt)_2$ [29] and $(C_2H_5)_4N[Ni(S_2COEt)_3]$ [19] were prepared by the literature methods. $(n\text{-}C_4H_9)_4N(BF_4)$ was purchased from Aldrich and

† Part of this work was presented at the NATO ASI Conference, 15–26 June, 1996, Przesieka, Poland.
‡ Present address: Department of Chemistry, Bilkent University, Ankara, Turkey.
§ Present address: Faculty of Engineering, Atılım University, Ankara, Turkey.

DOI: 10.1039/b105683m

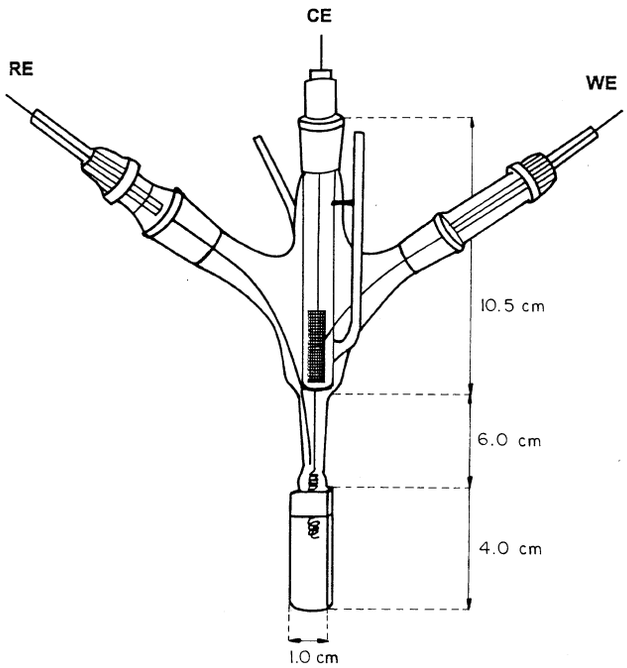


**Fig. 1** The apparatus used for measuring the *in situ* spectral changes during the constant potential electrolysis at room temperature; RE: Ag-wire reference electrode; CE: Pt-sieve counter electrode; WE: Pt-wire working electrode.

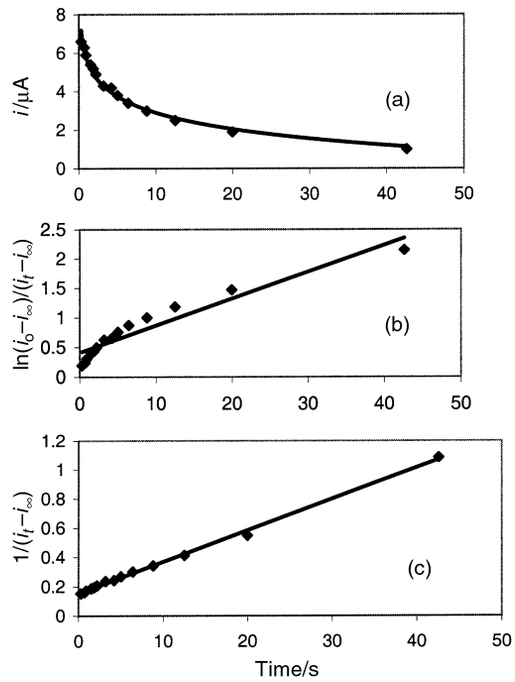


**Fig. 2** Decomposition kinetics of $[Ni^{III}(S_2COEt)_3]$ from CV measurements at 273 K. (a) The decay of the reduction peak current; (b) First order fit ($R^2 = 0.918$); (c) Second order fit ($R^2 = 0.997$).

used as supporting electrolyte without further purification. Iodine and potassium cyanide used were reagent quality. Acetonitrile, which was used as solvent, was Aldrich spectroscopic grade. The quantitative electronic absorption spectra[28] were used for identification. The elemental analysis for each compound was satisfactory.

Voltammetric recordings were made with a Lloyd PL3 XY/t recorder. A Pt-bead working, Pt-wire counter and an $Ag/Ag^+$ (0.10 M) reference electrode were used for CV studies. These three electrodes were positioned as close as possible to minimize IR drop. Cyclic voltammograms were recorded under a nitrogen atmosphere in acetonitrile at room temperature. Controlled potential electrolysis at the anodic peak potentials, were carried out with an Ag-wire reference electrode using the apparatus shown in Fig. 1. Both reference electrodes were calibrated against a ferrocene/ferrocenium couple, the oxidation potential was found to be 0.02 V *versus* $Ag/Ag^+$ (0.10 M) and 0.52 V *versus* Ag-wire. Oxidation processes have been followed *in situ* on a Hewlett-Packard UV-VIS HP 8452A diode array spectrophotometer. An FTIR Nicolet 510 spectrometer was also used for characterization of the compounds.

The rate of the decomposition reaction of $[Ni^{III}(S_2COEt)_3]$ formed by the electrochemical oxidation of $[Ni(S_2COEt)_3]^-$, was studied using CV and EPR methods.

### CV method

The $[Ni^{III}(S_2COEt)_3]$ complex was produced by electrolysis in a CV cell. The anodic scan (50 mV $s^{-1}$) started at −0.40 V and stopped at −0.15 V, which is the reversible oxidation peak potential for $[Ni(S_2COEt)_3]^-$, and the electrolysis was carried out for 60 s. After the electrolysis, the cycle (between 0.00 V and −0.40 V) was completed at different scan rates. Since the scan rate between −0.40 V and −0.15 V, electrolysis time and the concentration of $[Ni(S_2COEt)_3]^-$ were kept constant, the concentration of $[Ni^{III}(S_2COEt)_3]$ produced each time should also be the same. Completing the cycle at different scan rates gives different reduction peak heights, which reflects the different concentrations of the remaining $[Ni^{III}(S_2COEt)_3]$ species in solution. This allowed us to study the kinetics of the decomposition reaction. The decay of the reduction peak current with time, at 273 K, is presented in Fig. 2(a). To find the order of the decomposition reaction with respect to $[Ni^{III}(S_2COEt)_3]$, first $\ln(i_0 - i_\infty)/(i_t - i_\infty)$ and then $1/(i_t - i_\infty)$ *versus* time graphs were plotted using the same data, where $i_0$ and $i_\infty$ values are obtained by plotting the cathodic peak heights *versus* time (*i.e.* time intervals between the anodic and cathodic peaks on the voltammogram). This experiment was performed at three different temperatures, 253, 273 and 297 K. The plots for the decomposition reaction at 273 K are shown in Fig. 2(b) and 2(c) as examples.

### EPR method

The dichloromethane solution of $(C_2H_5)_4N[Ni(S_2COEt)_3]$ in the EPR cell is electrolyzed for 60 s using constant current (10 μA). EPR measurements were made on a Varian E12 EPR spectrometer. After the electrolysis stopped, the signal height was measured at different time intervals. The rate of the decomposition reaction was studied by following the decay of the EPR signal with time. This experiment was carried out at 231, 238, 245, and 258 K. The EPR signal obtained during the electrolysis at 245 K is shown in Fig. 3(a) and a representative example for $\ln((\text{signal height})_0/(\text{signal height})_t)$ and $1/(\text{signal height})_t$ *versus* time plots are given in Fig. 3(b) and 3(c), respectively.

## Results and discussion

### Oxidation of $K(S_2COEt)$

The cyclic voltammogram of $K(S_2COEt)$ in acetonitrile shows an irreversible oxidation peak at around 0.00 V referenced to $Ag/Ag^+$ electrode (Fig. 4(a)). Electrochemical oxidation has been carried out in $CH_3CN$ at this potential and the spectral changes are followed *in situ* on a UV-VIS spectrophotometer. The spectral changes during the constant potential electrolysis are shown in Fig. 5(a). The most intense band at 308, as well as the band at 226 nm in the spectrum[28] of $S_2COEt^-$ are diminished, while the two new bands at 286 and 246 nm are gradually developed. These bands are characteristic of the oxidized dimer form of the ethylxanthate ligand, $(S_2COEt)_2$. The isosbestic points at 290 and 240 nm clearly indicate a one-step reaction,

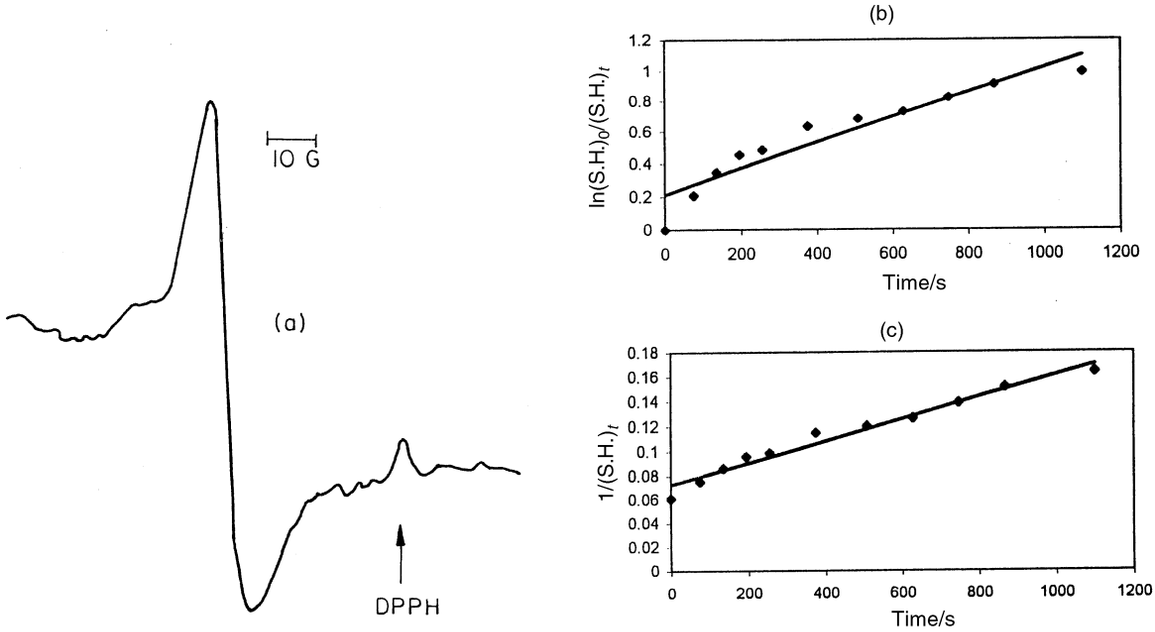


**Fig. 3** (a) EPR spectrum of $[Ni^{III}(S_2COEt)_3]$ measured at 245 K; (b) Decay of EPR signal at 245 K, first order fit ($R^2 = 0.901$); (c) Decay of EPR signal at 245 K, second order fit ($R^2 = 0.967$).

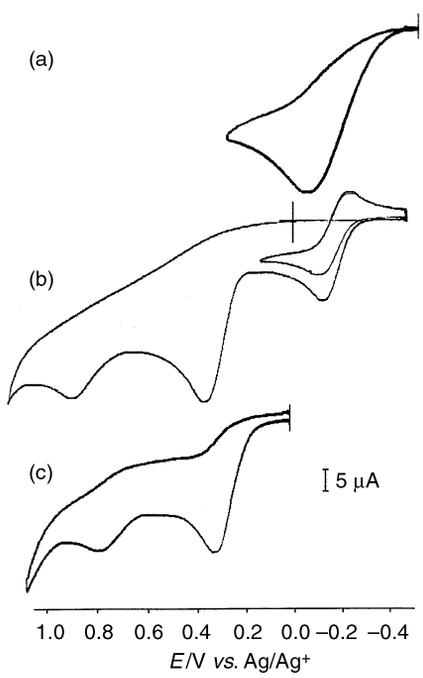


**Fig. 4** Cyclic voltammograms of (a) $K(S_2COEt)$; (b) $(Et_4N)[Ni(S_2COEt)_3]$; and (c) $Ni(S_2COEt)_2$, in acetonitrile–$(n\text{-}C_4H_9)_4N(BF_4)$ solvent–electrolyte couple at a voltage scan rate of 200 mV $s^{-1}$.

leading to the formation of $(S_2COEt)_2$ in the electrolysis solution. This observation is consistent with one electron oxidation of ethyl xanthate anion forming a radical followed by fast dimerization to form disulfide(dimer) as in eqn. (1) and (2).

$$S_2COEt^- \longrightarrow S_2COEt^{\bullet} + e^- \quad (1)$$

$$2S_2COEt^{\bullet} \longrightarrow (S_2COEt)_2 \quad (2)$$

The chemical oxidation of $S_2COEt^-$ by molecular iodine in $CH_3CN$ also gives the same spectral changes (the isosbestic point at 290 nm and the formation of the band at 286 nm), Fig. 5(b). In this process $S_2COEt^-$ is oxidized and $I_2$ is reduced to yield $(S_2COEt)_2$ and $I^-$ ion, respectively. However, the formation of $I^-$, which strongly absorbs in the UV region of the spectrum, influences the appearance of the higher energy part of the absorption spectrum of $(S_2COEt)_2$ ($I^-$ has absorption peaks at 246 ($\varepsilon = 15300$ $cm^{-1}$ $M^{-1}$) and 206 nm ($\varepsilon = 20600$ $cm^{-1}$ $M^{-1}$) in acetonitrile).

Our further investigation shows that the electrochemically generated dimer undergoes reduction with $CN^-$ (Fig. 5(c)) as in eqn. (3).

$$(S_2COEt)_2 + 2CN^- \longrightarrow 2S_2COEt^- + (CN)_2 \quad (3)$$

Comparison of the changes in the absorption spectra given in Fig. 5, indicate that the electrochemical and chemical oxidation of ethyl xanthate anion yields the same product, and it is also possible to reverse the oxidation by $CN^-$ to regenerate the ethyl xanthate anion.

### Oxidation of $Ni(S_2COEt)_2$

There are two irreversible oxidation peaks in the cyclic voltammogram of $Ni(S_2COEt)_2$ in acetonitrile at 0.35 and 0.80 V *versus* Ag/Ag+ reference electrode (Fig. 4(c)). Constant potential electrolysis has been carried out at the first peak potential. The spectral changes during the electrolysis of about $10^{-5}$ M $Ni(S_2COEt)_2$ are shown in Fig. 6. The bands at 414, 474, 316 and 218 nm, which are characteristic bands in the spectrum of $Ni(S_2COEt)_2$[28] gradually lose their intensities, as the bands at 286 and 246 nm, originating from $(S_2COEt)_2$, intensify with time during the electrolysis. Two sharp isosbestic points at 290 and 224 nm are observed. The final spectrum is consistent with that of $(S_2COEt)_2$. This result suggests that oxidation is taking place as in eqn. (4). At this concentration the presence of $Ni^{2+}$

$$Ni(S_2COEt)_2 \longrightarrow Ni^{2+}(sol) + (S_2COEt)_2 + 2e^- \quad (4)$$

ion in solution is not detectable from the electronic absorption spectrum, because the d–d absorption of the hexaacetonitrile-nickel(II) complex is very weak.[30] The presence of $Ni^{2+}$ ion in solution has been demonstrated by titration of the electrolyzed solution with $CN^-$, which yielded the $[Ni(CN)_4]^{2-}$ complex,[31] xanthate ligand, and cyanogen according to eqn. (5).

$$Ni^{2+}(sol) + (S_2COEt)_2 + 6CN^- \longrightarrow [Ni(CN)_4]^{2-} + 2S_2COEt^- + (CN)_2 \quad (5)$$

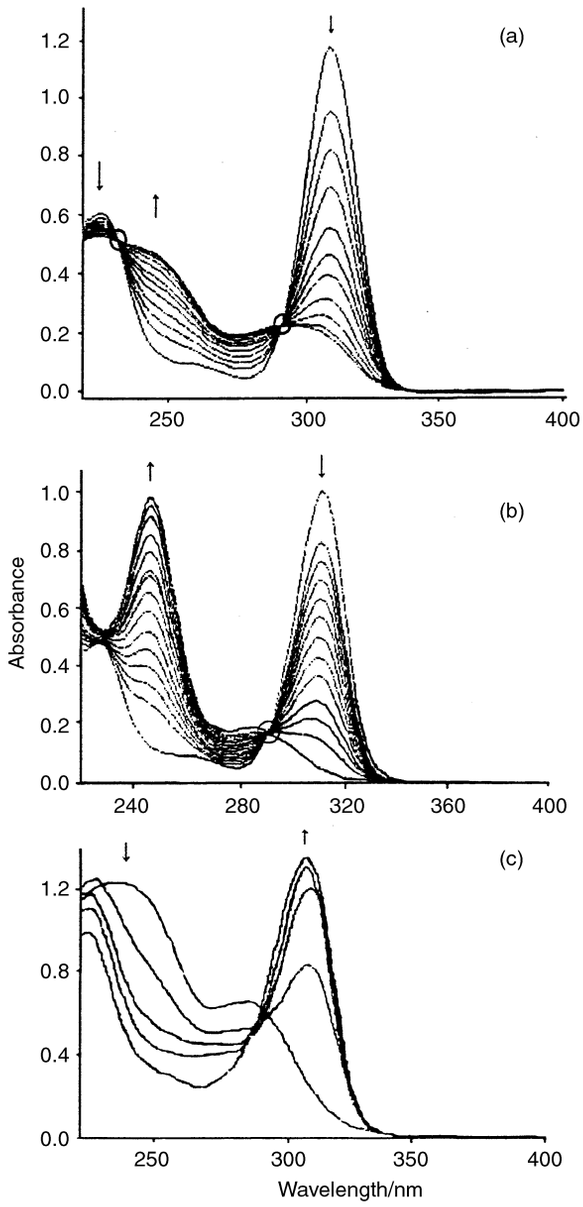


**Fig. 5** UV-VIS absorption spectral changes during (a) constant potential electrolysis of a $5 \times 10^{-5}$ M solution of $K(S_2COEt)$ (there are 5 min intervals between scans), (b) chemical oxidation of $K(S_2COEt)$ with $I_2$, and (c) chemical reduction of $(S_2COEt)_2$ with $CN^-$ in acetonitrile.

When the acetonitrile solution of $Ni(S_2COEt)_2$ was titrated with saturated KCN solution (such that the volume change is negligible during titration) and absorption spectral changes were measured *in situ*, a set of sharp isosbestic points were observed until the mole ratio of $CN^-/Ni^{2+}$ was 4/3. These isosbestic points were lost upon addition of more $CN^-$ and a new set developed. The spectrum of the solution at the end was the same as the overlapped spectrum of $[Ni(CN)_4]^{2-}$ and $K(S_2COEt)$ in acetonitrile. These experimental results are interpreted as two consequent reactions as in eqn. (6) and (7).

$$3Ni(S_2COEt)_2 + 4CN^- \longrightarrow [Ni(CN)_4]^{2-} + 2[Ni(S_2COEt)_3]^- \quad (6)$$

$$2[Ni(S_2COEt)_3]^- + 8CN^- \longrightarrow 2[Ni(CN)_4]^{2-} + 6S_2COEt^- \quad (7)$$

**Oxidation of $(NEt_4)[Ni(S_2COEt)_3]$**

The cyclic voltammogram of $(NEt_4)[Ni(S_2COEt)_3]$ in acetonitrile displays one reversible, at −0.15 V, and two irreversible, at 0.35 and 0.80 V, oxidation peaks *versus* the $Ag/Ag^+$ reference electrode (Fig. 4(b)). Constant potential electrolysis of this complex in acetonitrile was performed at the lowest oxidation peak potential. The absorption spectral changes, which were measured *in situ* during the electrolysis, are presented in Fig. 7(a). Seven isosbestic points are observed as the bands due to the starting complex disappeared and the characteristic bands of $Ni(S_2COEt)_2$ developed. The final spectrum is the same as the one obtained from the 1 : 2 mixture of $(S_2COEt)_2$

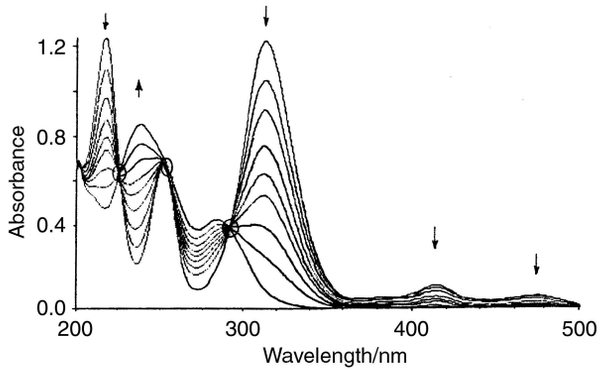


**Fig. 6** UV-VIS absorption spectral changes during the constant potential electrolysis of a $3 \times 10^{-5}$ M solution of $Ni(S_2COEt)_2$ in acetonitrile. (There are 5 min intervals between scans.)

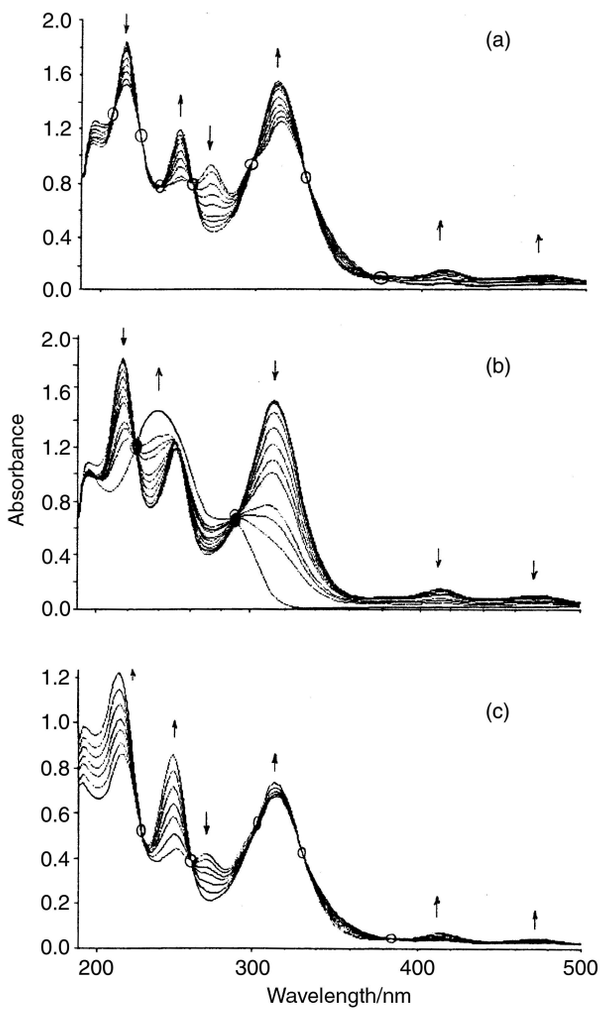


**Fig. 7** UV-VIS absorption spectral changes during, (a) the constant potential electrolysis of $[Et_4N][Ni(S_2COEt)_3]$ at the first oxidation peak potential (there are 5 min intervals between scans); (b) followed, at the second oxidation peak potential (5 min intervals between scans); and (c) the chemical oxidation of $[Et_4N][Ni(S_2COEt)_3]$ by $I_2$ in acetonitrile.

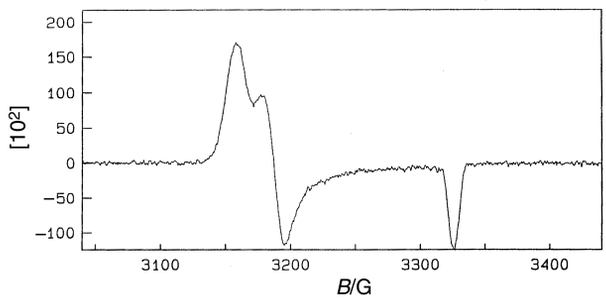


**Fig. 8** EPR spectrum of $[Ni^{III}(S_2COEt)_3]$ in acetonitrile at 10 K. (Frequency = 9.4653600 GHz.)

and $Ni(S_2COEt)_2$. This observation indicates that the oxidation of $[Ni(S_2COEt)_3]^-$ at a potential corresponding to the lowest oxidation peak potential in its cyclic voltammogram, yields $Ni(S_2COEt)_2$, and $(S_2COEt)_2$, as the final products. Our room temperature *in situ* measured UV-VIS spectral data do not show any sign of intermediate formation during the oxidation process. However, the *in situ* electrolysis of a dichloromethane solution of $(C_2H_5)_4N[Ni(S_2COEt)_3]$ in an EPR cell, at low temperature, yielded a singlet with a "*g*" value of 2.09 as shown in Fig. 3(a). We have also measured the EPR spectrum of the acetonitrile solution of tris(ethylxanthato)nickel(II) at 10 K,[32] after constant potential electrolysis at 253 K. This spectrum is presented in Fig. 8.

The EPR spectrum clearly indicates the formation of an Ni(III) species in the oxidative electrolysis process. Thus, the reversible peak obtained on the voltammogram corresponds to an Ni(II)/Ni(III) redox couple. Since no absorbance due to the Ni(III) species[24] has been recorded by *in situ* UV-VIS measurements during the room temperature electrolysis, the $[Ni^{III}(S_2COEt)_3]$ complex formed at the electrode surface must decompose to the observed final products before it reaches the light path in the UV cell. Therefore, the mechanism of the electrochemical oxidation process at the first oxidation peak potential can be represented by eqn. (8)–(10); where an electron

$$[Ni(S_2COEt)_3]^- \rightleftharpoons [Ni^{III}(S_2COEt)_3] + e^- \quad (8)$$

$$[Ni^{III}(S_2COEt)_3] \underset{k_{-1}}{\overset{k_1}{\rightleftharpoons}} [Ni^{II}(S_2COEt)_2(S_2COEt^{\bullet})] \quad (9)$$

$$2[Ni^{II}(S_2COEt)_2(S_2COEt^{\bullet})] \xrightarrow{k_2} 2Ni(S_2COEt)_2 + (S_2COEt)_2 \quad (10)$$

is reversibly removed from the tris(ethylxanthato)nickel(II) anion forming $[Ni^{III}(S_2COEt)_3]$, which yields a radical complex, $[Ni^{II}(S_2COEt)_2(S_2COEt^{\bullet})]$, in a rapid equilibrium step. The radical complex undergoes a bimolecular reaction to yield $Ni(S_2COEt)_2$ and $(S_2COEt)_2$ as final products.

Further controlled potential oxidative electrolysis of the above electrolyzed solution was carried out at the second oxidation peak potential. Spectral changes during the second electrolysis are shown in Fig. 7(b). The spectral changes displayed in this figure and in Fig. 6, which displays the spectral changes observed during the electrolysis of $Ni(S_2COEt)_2$, are strikingly similar. Two sharp isosbestic points at 290 and 224 nm are common to both. These results leave no doubt that the $Ni(S_2COEt)_2$ complex formed at the end of the electrolysis at the first oxidation peak potential, is further oxidized to produce $Ni^{2+}$(sol) and the dimer of the oxidized ligand, as shown in eqn. (4).

The chemical oxidation of $[Ni(S_2COEt)_3]^-$ in acetonitrile was also carried out with iodine. The spectral changes measured during the titration of $[Ni(S_2COEt)_3]^-$ with a concentrated acetonitrile solution of $I_2$ (Fig. 7(c)), are very similar to that of the electrochemical oxidation at the first peak potential (Fig. 7(a)). The differences around 246 and 206 nm are due to the absorption of $I^-$ ion. This observation suggests that both electrochemical and chemical oxidation yield the same final products.

The electrochemical oxidation of $[Ni(S_2COEt)_3]^-$ was studied by Chakravorty *et al.*[27] Their experimental observations were similar to ours. The equilibrium constant for the decomposition reaction of $[Ni^{III}(S_2COEt)_3]$ to $Ni(S_2COEt)_2$ and $(S_2COEt)_2$ was calculated to be 391 M at 298 K. The rate of the decomposition reaction of nickel(III) complex was claimed to be first order with a rate constant of $1.0 \times 10^{-3}$ $s^{-1}$ at 253 K; and the activation entropy, $\Delta S^*$, was found to be about −40 eu. In fact, we have also found a negative entropy of activation both from the CV (≈ −46 eu) and EPR method (≈ −60 eu). If the decomposition reaction rate is first order with respect to $[Ni^{III}(S_2COEt)_3]$, the activation step in the proposed mechanism would be the formation of $[Ni^{II}(S_2COEt)_2(S_2COEt^{\bullet})]$ complex radical from $[Ni^{III}(S_2COEt)_3]$. It is very difficult to visualize how an electron transfer from a ligand to the nickel center results in such a large decrease in entropy. The large negative entropy of activation can be explained by a mechanism whereby the $[Ni^{III}(S_2COEt)_3]$ decomposes to $Ni(S_2COEt)_2$ and $(S_2COEt)_2$ as shown in the following scheme:

$$2[Ni^{III}(S_2COEt)_3]$$

$$\downarrow\uparrow$$

$$2\,[Ni^{II}(S_2COEt)_2\,(S_2COEt^{\bullet})]$$

$$\downarrow$$

$$\{Ni^{II}(S_2COEt)_2\,(S_2COEt^{\bullet})\text{-----}(^{\bullet}S_2COEt)(S_2COEt)_2Ni^{II}\}$$

ACTIVATED COMPLEX

$$\downarrow$$

$$2Ni(S_2COEt)_2 + (S_2COEt)_2$$

The above mechanistic scheme is a manifestation of eqn. (9) and (10). The rate law expression for the decomposition of $[Ni^{III}(S_2COEt)_3]$ to $Ni(S_2COEt)_2$ and $(S_2COEt)_2$, can be derived using a rapid equilibrium assumption and has the following form:

$$-\frac{d[Ni^{III}(S_2COEt)_3]}{dt} = k[Ni^{III}(S_2COEt)_3]^2,$$

$$\text{where: } k = \frac{2k_2K_1^2}{(K_1+1)}, \quad K_1 = \frac{k_1}{k_{-1}}$$

Since we have detected the presence of nickel(III) species by EPR at low temperature, and by CV at room temperature, the rapid equilibrium must mainly lie to the left. This implies that $K_1 << 1$, and $k = 2k_2K_1^2$. If our proposed mechanism is correct then the rate of the decomposition reaction must be second order with respect to $[Ni^{III}(S_2COEt)_3]$. In order to check this hypothesis we followed the decay kinetics of nickel(III) species using EPR and CV methods as described in the experimental section. The kinetic data obtained from EPR and CV experiments gave a better fit to a second order integrated rate law, rather than the first order one (see Fig. 2 and 3). It was also very clear from our data that the half-lives of the decay reaction of the nickel(III) species were initial concentration dependent (Fig. 2(a)). Both half-life and Wilkinson[33] methods also suggested a second order decay reaction. All these observations are consistent with our proposed mechanism, in which the rate determining step is the bimolecular reaction of the radical complex (eqn. (10)), yielding a large negative entropy of activation.

## Conclusion

The lowest oxidation peaks in the cyclic voltammograms of $S_2COEt^-$, $Ni(S_2COEt)_2$, and $[Ni(S_2COEt)_3]^-$ appear at 0.00, 0.35, and −0.15 V, respectively, *versus* $Ag/Ag^+$ reference electrode in acetonitrile. The oxidation peak for $[Ni(S_2COEt)_3]^-$ is reversible. Constant potential electrolysis carried out at potentials corresponding to the above peak potentials for each species, always yielded $(S_2COEt)_2$ as one of the final products. The chemical oxidation of $S_2COEt^-$ and $[Ni(S_2COEt)_3]^-$ with $I_2$ resulted in the same final products as the electrochemical oxidation.

The electrochemical oxidation of $[Ni(S_2COEt)_3]^-$ by constant potential electrolysis at the first oxidation peak potential resulted in the nickel(III) species, which then decomposed to $Ni(S_2COEt)_2$ and $(S_2COEt)_2$ as the final products. The kinetic data obtained in this work suggest that the decomposition reaction is second order with respect to $[Ni^{III}(S_2COEt)_3]$.

In this study, we have demonstrated that electrochemical and chemical oxidation–reduction processes can be followed by *in situ* UV-VIS spectrophotometry to identify the final products of the process if the absorption spectra of the expected products are known. However, it may not be possible to obtain a real picture if the lifetime of the redox species are not long enough.

## Acknowledgements

We would like to thank Middle East Technical University Research Fund and Project TBAG-1520 for support of this work.

## References

1 K. Nag and A. Chakravorty, *Coord. Chem. Rev.*, 1980, **3**, 87.
2 P. Schoneit, J. Moll and R. K. Thauer, *Arch. Microbiol.*, 1979, **123**, 105.
3 W. Kaim and B. Schwederski, *Bioinorganic Chemistry: Inorganic Elements in the Chemistry of Life*, John Wiley & Sons, New York, 1994.
4 R. Cammack, *Adv. Inorg. Chem.*, 1988, **32**, 297.
5 J. J. Moura, M. Teixeira and I. Moura, *Pure Appl. Chem.*, 1989, **61**, 915.
6 A. Volbeda, M. H. Charon, C. Piars, E. C. Hatchikian, M. Frey and J. C. Fontecilla-Camps, *Nature*, 1995, **373**, 580.
7 M. Kumar, R. O. Day, G. J. Colpas and M. J. Maroney, *J. Am. Chem. Soc.*, 1989, **111**, 5974.
8 A. R. Hendrickson, R. L. Martin and N. M. Rohde, *Inorg. Chem.*, 1975, **14**, 2980.
9 R. I. Haines and A. McAuley, *Coord. Chem. Rev.*, 1981, **39**, 77.
10 E. S. Gore and D. H. Bush, *Inorg. Chem.*, 1973, **12**, 1.
11 L. Fabbrizzi, T. A. Kaden, A. Perotti, B. Seghi and L. Siegfried, *Inorg. Chem.*, 1986, **25**, 321.
12 S. Bhattacharya, R. Mukherjee and A. Chakravorty, *Inorg. Chem.*, 1986, **25**, 3448.
13 A. G. Lappin and A. McAuley, *Adv. Inorg. Chem.*, 1988, **32**, 241.
14 H. J. Kruger, G. Peng and R. H. Holm, *Inorg. Chem.*, 1991, **30**, 734.
15 J. D. Franolic, W. Y. Wang and M. Millar, *J. Am. Chem. Soc.*, 1992, **114**, 6587.
16 S. Mukhopadhyay and D. Ray, *J. Chem. Soc., Dalton Trans.*, 1995, 265.
17 F. P. Bossu and D. W. Margerum, *Inorg. Chem.*, 1977, **16**, 1210.
18 J. J. Czarnecki and D. W. Margerum, *Inorg. Chem.*, 1977, **16**, 1997.
19 D. Coucouvanis and J. P. Fackler, *Inorg. Chem.*, 1967, **6**, 2047.
20 D. M. Dooley and B. M. Patterson, *Inorg. Chem.*, 1982, **21**, 4330.
21 A. Vogler, H. Kunkely, J. Hlavatsch and A. Mers, *Inorg. Chem.*, 1984, **23**, 506.
22 J. P. Fackler, A. Avdeef and R. G. Fischer, *J. Am. Chem. Soc.*, 1973, **95**, 774.
23 W. Rosen and D. H. Busch, *J. Am. Chem. Soc.*, 1969, **91**, 4694.
24 H.-J. Kruger and R. H. Holm, *J. Am. Chem. Soc.*, 1990, **112**, 2955.
25 M. A. Halcrow and G. Christou, *Chem. Rev.*, 1994, **94**, 2421.
26 J. Hanss and H.-J. Kruger, *Angew. Chem., Int. Ed.*, 1998, **37**, 360.
27 S. B. Choudhury, D. Ray and A. Chakravorty, *Inorg. Chem.*, 1990, **29**, 4603.
28 H. Isci, O. Dag and W. R. Mason, *Inorg. Chem.*, 1993, **32**, 3909.
29 G. W. Watt and B. J. J. McCormick, *Inorg. Chem.*, 1965, **27**, 898.
30 B. J. Hathaway and D. G. Holah, *J. Chem. Soc.*, 1964, 2400.
31 S. B. Piepho, P. N. Schatz and A. J. McCaffery, *J. Am. Chem. Soc.*, 1969, **91**, 5994.
32 The EPR spectrum at 10 K was measured at MPI für Strahlenchemie, Müelheim, Germany and added during the revision.
33 J. H. Espenson, *Chemical Kinetics and Reaction Mechanisms*, 2nd. edn., McGraw-Hill, Inc., New York, 1995.